Mechanisms of conduit plug formation: Implications for vulcanian explosions

K. Diller,[1] A. B. Clarke,[1] B. Voight,[2] and A. Neri[3]

Received 28 June 2006; revised 22 August 2006; accepted 14 September 2006; published 17 October 2006.

[1] We explore physical mechanisms controlling formation of a confining conduit plug using 1D, steady-state numerical models of magma ascent. Model results for the well-documented 1997 Vulcanian explosions at Soufrière Hills volcano were compared against subsurface conditions constrained by geophysical and petrologic analysis. We suggest that, if magma is permeable and overpressured and rock surrounding the conduit is permeable, degassing occurs both vertically and through conduit walls. This outgassing creates a region of low-vesicularity, dense magma near the surface (*magma plug*) which eventually seals the conduit and promotes system overpressure. Driving pressure increases with increasing magma flow rate, hindering volatile exsolution and shifting open-system degassing to shallower levels of the conduit. As a result, increasing magma flow rate for a fixed conduit width creates a vertically thinner plug and increases the magnitude and vertical extent of conduit overpressure. Plug thickness and density are also controlled by magma and edifice permeability. **Citation:** Diller, K., A. B. Clarke, B. Voight, and A. Neri (2006), Mechanisms of conduit plug formation: Implications for vulcanian explosions, *Geophys. Res. Lett.*, *33*, L20302, doi:10.1029/2006GL027391.

1. Introduction

[2] Vulcanian eruptions are short-lived explosions resulting from sudden decompression of a conduit containing high-pressure, vesiculated magma. Typically Vulcanian eruptions last only seconds to minutes and erupt <0.1 km^3 of magma [*Morrissey and Mastin*, 2000]. Dense, ballistic blocks commonly associated with Vulcanian eruptions are evidence of a degassed, crystalline magma plug residing in the upper conduit prior to an explosion which may have sealed the system and promoted high conduit overpressure [*Hammer et al.*, 1999; *Belousov et al.*, 2002; *Druitt et al.*, 2002; *Taddeucci et al.*, 2004; *Cashman and McConnell*, 2005; *D'Oriano et al.*, 2005]. A magma plug may form due to: 1) exsolution of volatiles and microlite crystallization, both of which increase bulk magma viscosity and strength [*Sparks*, 1997; *Stix et al.*, 1997] and 2) gas escape from the conduit which leads to vesicle collapse and magma densification [*Hammer et al.*, 1999; *Taddeucci et al.*, 2004; *Cashman and McConnell*, 2005; *D'Oriano et al.*, 2005].

[3] One-dimensional, steady-state conduit models have proven useful for discerning a variety of volcanic eruption phenomena, including lava dome extrusion [*Melnik and Sparks*, 1999, 2002a] and transitions between effusive and explosive eruptions [*Melnik and Sparks*, 2002b; *Melnik et al.*, 2005]. Here we focus on elucidating the subsurface processes that contribute to magma plug formation, particularly within cycles of Vulcanian explosions. Although we follow the model of *Melnik and Sparks* [1999], we extend it by incorporating degassing through conduit walls, enabling exploration of three conceptual models of plug formation and sensitivity of plug characteristics and conduit overpressure to magma rheology, magma flow rate, and system permeability.

2. Conduit Model

[4] For all models, the conduit is assumed to be a vertical cylinder of constant diameter D and length L. At depth L, magma enters the conduit from the chamber with crystal volume fraction β and total gas mass fraction x_{tot} and ascends at flow rate Q reaching the surface at atmospheric pressure. Magma density and viscosity change due to melt degassing during ascent, which we assume occurs instantaneously in response to decompression and thus equilibrium is maintained. Conceptually, magma rises steadily to fill the emptied conduit following an explosion and stagnates beneath a magma plug until the next explosion. Here we consider only magma ascent between explosions in order to predict the stagnated, pre-explosion conduit profile. The highly unsteady transition between magma ascent and Vulcanian explosion is not addressed in this study, but the reader can refer to *Melnik and Sparks* [2002b] and *Melnik et al.* [2005] for further insight into the transition.

[5] The conservation of mass for both the magma (melt and crystals) and gas (dissolved and exsolved portions) (modified from *Melnik and Sparks* [1999]) are:

$$\frac{d}{dz}\rho V = \frac{d}{dz}Q = 0 \tag{1}$$

$$\frac{d}{dz}\rho_g \alpha V_g + \frac{d}{dz}\rho_{xd} V = \frac{d}{dz}Q_g = Q_{gloss} \tag{2}$$

$$\rho = (1-\alpha)(\rho_m(1-\beta)(1-x_d) + \rho_c\beta) \tag{3}$$

$$\rho_{xd} = \rho_m(1-\alpha)(1-\beta)x_d \tag{4}$$

$$Q_{gloss} = \frac{2\rho_g \alpha k_{cr}(p - p_{lith})}{\mu_g \left(\frac{D}{2}\right)^2} \tag{5}$$

[1] School of Earth and Space Exploration, Arizona State University, Tempe, Arizona, USA.
[2] College of Earth and Mineral Sciences, Pennsylvania State University, University Park, Pennsylvania, USA.
[3] Sezione di Pisa, Istituto Nazionale di Geofisica e Vulcanologia, Pisa, Italy.

0094-8276/06/2006GL027391$05.00

Here z is height above the chamber, α is the gas volume fraction in the whole mixture (melt, crystals, and exsolved gas), β is the crystal volume fraction in the magma, x_d is the mass concentration of dissolved gas in the melt, ρ, ρ_m, ρ_c, ρ_g, and ρ_{xd} are the densities of the magma, melt, crystals, gas, and dissolved gas, respectively, μ_g is the viscosity of the gas phase, D is the conduit diameter, k_{cr} is the permeability of the surrounding country rock, p and p_{lith} are mixture and lithostatic pressure at a given depth, V and V_g are the velocities of the magma and gas, Q and Q_g are the discharge rates of magma and gas per unit of cross-sectional area, and Q_{gloss} is a sink term accounting for gas loss through conduit walls. We assume that expansion of exsolved gas is limited by pressure, not by magma viscosity, and therefore magma and gas pressures are equal. *Melnik et al.* [2005] explore the effects of differential gas and magma pressure on the transition from effusive to explosive eruption.

[6] Previous studies suggest that significant gas loss through shallow conduit walls occurs, perhaps enhanced by the presence of fractures in the volcanic edifice [*Heiken et al.*, 1988; *Jaupart and Allègre*, 1991; *Widiwijayanti et al.*, 2005], prompting incorporation of the gas loss term in equation (5). Gas loss is permitted through conduit walls only where two criteria are met: conduit pressure with respect to lithostatic pressure is greater than zero (overpressured), and magma vesicularity is sufficient for bubble connectivity. Bubble connectivity occurs at ~60% porosity (based on natural samples [*Eichelberger et al.*, 1986]) or between 45–80% porosity (based on experimental samples [*Takeuchi et al.*, 2005]). We assume a connectivity threshold of 60% porosity, but test a range of values from 45–80%. Due to the alignment and coalescence of bubbles and fracturing, permeable networks and pathways for gas escape persist even as magma porosity decreases due to open-system degassing [*Saar and Manga*, 1999; *Takeuchi et al.*, 2005]. We therefore assume that permeability does not decrease as the volatile phase leaves the system and bubbles collapse (that is, until porosity is significantly reduced and sealing occurs).

[7] The conservation of momentum for the mixture takes the form:

$$\frac{d}{dz}p = -\rho_{mix}g - \frac{32\mu_{mix}V}{D^2} \tag{6}$$

where ρ_{mix} is the density of the mixture, g is acceleration due to gravity, and μ_{mix} is the viscosity of the mixture. Viscous forces take a modified Poiseuille form for fully developed laminar flow in a pipe. Inertial terms are negligibly small relative to viscous and gravitational forces and are therefore neglected. The viscosity of the mixture is a function of melt viscosity and crystal volume fraction, using a fit of SHV dome rock data [*Melnik and Sparks*, 1999, equations (6) and (8)], where the viscosity of the melt phase μ_m is a function of temperature T and the mass fraction of water dissolved in the melt x_d [*Hess and Dingwell*, 1996].

[8] An increase of bubble volume fraction from 0 to 0.50 decreases mixture viscosity by only a factor of three [*Lejeune et al.*, 1999], whereas melt degassing changes mixture viscosity by four orders of magnitude over the length of the modeled conduits presented here. Furthermore, our model solutions fall in the dynamic transition zone of *Llewellin and Manga* [2005], making their step-function method of accounting for bubbly rheology inappropriate. We therefore ignore the effects of bubbles on mixture viscosity and further discuss this assumption later in the text.

[9] Magma porosity allows the condensed and gas phases to move at different vertical velocities, provided that magma permeability is sufficient for gas to flow through the bubbly magma. Assuming Darcian flow through porous media, V_g is related to V via vertical permeability k, gas viscosity μ_g, and vertical pressure gradient dp/dz, as follows

$$V_g - V = \frac{k(k_0, \alpha)}{\mu_g}\frac{d}{dz}p \tag{7}$$

Permeability k varies as a function of gas volume fraction α and coefficient k_0 according to *Melnik and Sparks* [1999, equation [7]], following from *Klug and Cashman* [1996].

[10] Equations (6) and (7) were combined to obtain an equation for $d\alpha/dz$. Equation (6) and the new equation were solved simultaneously using a fourth-order Runge-Kutta scheme with variable step-size. We tested an initial chamber pressure and the conduit profile was solved between the magma chamber and surface. Magma viscosity and density were updated after each spatial step using the new values of p and α. Chamber pressure was adjusted and the process repeated until the exit boundary condition (atmospheric pressure) was satisfied.

[11] Here we apply the model to the well-documented 1997 sequence of Vulcanian explosions at Soufrière Hills volcano (SHV), Montserrat, but the overall relationships are general and may be applied to any volcanic system. The chamber depth is taken as 5 km [*Barclay et al.*, 1998], the conduit diameter as 30 m [*Voight et al.*, 1999], the total gas mass fraction in the chamber as 0.043 [*Barclay et al.*, 1998], the crystal volume fraction in the magma as 0.45 [*Murphy et al.*, 1998], the melt density as 2300 kg m^{-3}, and the crystal density as 2700 kg m^{-3}. The gas phase is assumed ideal and the system isothermal [as in *Wilson et al.*, 1980] at 860°C [*Barclay et al.*, 1998; *Murphy et al.*, 1998]. The mass fraction of water dissolved in the melt is $x_d = sp^{\frac{1}{2}}$, where, for the SHV rhyolitic melt [*Murphy et al.*, 1998] $s = 4.1 \times 10^{-6}$ $N^{\frac{1}{2}}$ m^{-1} [*Wilson et al.*, 1980]. On average, the 1997 SHV Vulcanian events erupted 3×10^5 m^3 dense rock equivalent and had ten-hour repose periods, during which the average magma flow rate was ~7.5 m^3 s^{-1} [*Druitt et al.*, 2002].

3. Model Results

[12] We constrain our model results using two independent data sets from the 1997 Montserrat explosions. Clasts from the 1997 SHV events were analyzed and interpreted within the context of experimentally-derived relationships between groundmass textures and quench pressure (A. Clarke et al., Petrological constraints on the decompression history of magma prior to vulcanian explosions at the Soufrière Hills Volcano, Montserrat, submitted to *Journal of Volcanology and Geothermal Research*, 2006, hereinafter referred to as Clarke et al., submitted manuscript, 2006). The study led to a subsurface conduit profile (Figure 1a,

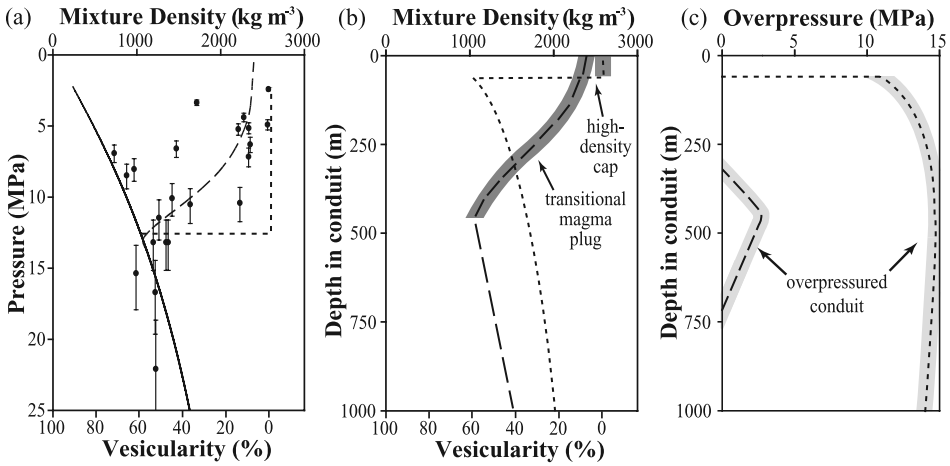

Figure 1. (a) Density vs. pressure for erupted clast samples (circles) [*Clarke et al.*, submitted manuscript, 2006] and pre-eruptive magma column profiles for Model A, $Q_{vol} = 7.5\ m^3\ s^{-1}$ with vertical degassing only (solid line); Model B, $Q_{vol} = 7.5\ m^3\ s^{-1}$ with vertical and conduit wall degassing (dashed line); and Model C, $Q_{vol} = 75\ m^3\ s^{-1}$ followed by vertical and conduit wall degassing of a static magma column (dotted line). (b) Density and (c) overpressure vs. depth in conduit for Model B (dashed line) and Model C (dotted line).

circles) revealing a trend of increasing density with decreasing depth in the shallow conduit. The very dense (low vesicularity) magma near the surface is thought to be the pre-eruptive representation of the dense ballistics ejected at the start of the SHV explosions [*Druitt et al.*, 2002]. Our model results of pressure and magma porosity can be compared against this subsurface conduit profile. Additionally, independent estimates of depth to source and magnitude of overpressure have been made from interpretation of near-field tilt data using Mogi, Boussinesq halfspace, and full topography 3D elastic models [*Voight et al.*, 1998; *Widiwijayanti et al.*, 2005], against which our overpressure estimates can be compared.

3.1. Models A and B: Steady Ascent and Degassing at Average Flow Rate

[13] Our first conceptual model assumes steady flow over the period between eruptions and uses the average volumetric flow rate of 7.5 $m^3\ s^{-1}$, estimated from field observations [*Druitt et al.*, 2002]. In Model A, continuous permeable gas loss in the vertical direction is allowed throughout the ascent process, but Q_{gloss} is set to zero. Results using vertical permeability coefficient $k_0 = 0.1$ (Figure 1a, solid line) provide the best fit of the lower conduit (greater than about 7 MPa) clast data (Clarke et al., submitted manuscript, 2006) (Figure 1a, circles). However, this model does not match the transition to the dense magma plug in the upper region of the conduit, leading to the conclusion that a magma plug cannot result from degassing in the vertical direction alone, given our assumed Darcian flow (equation (7)).

[14] Next, in Model B, we allow gas loss vertically and through conduit walls if the conduit is overpressured relative to the surrounding rock and magma porosity exceeds 60% (Figure 1, dashed line). Escape of volatiles through conduit walls, followed by vesicle collapse, leads to densification of magma in the upper conduit (less than about 13 MPa). A range of surrounding country rock permeabilities were tested (10^{-16}–$10^{-11}\ m^2$) [*Jaupart and Allègre*, 1991], and results using $k_{cr} = 4.8 \times 10^{-14}\ m^2$ provide a reasonable fit to the clast-derived conduit profile, such that at pressures less than about 13 MPa, magma becomes more dense with decreasing depth, creating a transitional magma plug and a shallow high-density zone (Figure 1a).

[15] Where magma pressure exceeds lithostatic and magma or conduit wall permeability is insufficient to fully dissipate gas overpressure via permeable gas loss, conduit overpressure is maintained. Model B suggests that for the 1997 SHV case, the overpressured zone extends from 300 to 750 m depth and has a maximum of 3 MPa at 450 m depth (Figure 1c). Pressure source depth and magnitude during an effusive phase of the SHV eruption were estimated using ratios of near-field tilt measurements and by assuming a Mogi source, with further evaluation by full topography 3D elastic models: *Voight et al.* [1998] estimated source depths of <600 m to 800 m, while *Widiwijayanti et al.* [2005] estimated magnitudes of 1–4 MPa at depths between 740 and 970 m. At depths greater than 700 m, the Model B conduit is underpressured with respect to lithostatic, consistent with calculations by *Melnik et al.* [2005], where the magma chamber becomes underpressured after explosive evacuation of the upper conduit and remains so as magma ascends in response to the unloading.

3.2. Model C: Rapid Ascent Followed by Degassing of Stagnated Magma

[16] The second conceptual model (Model C) assumes rapid magma ascent in response to unloading from the previous explosive event, followed by permeable degassing of a static magma column over the remainder of the ten-hour repose period. Steady magma ascent is again assumed, with volume flow rate increased by a factor of 10 ($75\ m^3\ s^{-1}$) to account for the shortened period of ascent. Once the magma column stagnates, gas loss occurs according to

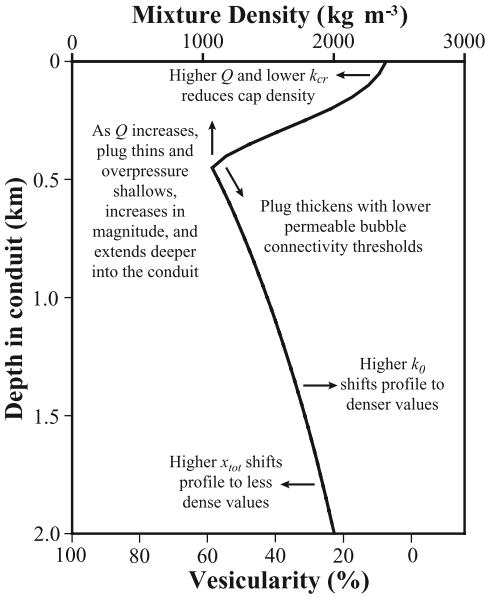

Figure 2. The sensitivity of degassed plug thickness and density to surrounding rock permeability k_{cr}, vertical permeability coefficient k_0, magma flux Q, total gas mass fraction x_{tot}, and permeable bubble threshold for Model B, shown as depth in conduit vs. magma mixture density.

standard flow through porous media (using the same k_{cr} as in Model B) where the bubble connectivity threshold is met and the conduit is overpressured with respect to lithostatic. Model C (Figure 1, dotted line) produces a 60 m thick, high-density plug or cap and lacks an underlying transitional zone as suggested by clast data and Model B. The plug is much thinner than that formed by Model B because pressures required to drive such a high flow rate decrease magma vesicularity, and thus the bubble connectivity threshold is satisfied only in the very shallow conduit, limiting the depth of open-system degassing. The plug does not have a transition zone because the stagnant, shallow magma completely degassed (open-system) over the duration of the repose period, resulting in only high-density magma. Model C produces significantly higher maintained overpressures (14 MPa), extending over a greater depth range (60–5000 m), than those produced by Model B (Figure 1c). The sharp boundary between a very dense plug and underlying highly vesicular magma is inconsistent with the transitional profile suggested by clast analysis (Figure 1a), and the extensive zone of high overpressure (Figure 1c) is incompatible with observed deformation which was estimated to be a result of shallow overpressures of 1 to 4 MPa [*Widiwijayanti et al.*, 2005].

3.3. Generalized Model Results

[17] The sensitivity of plug characteristics to system parameters in conceptual Model B is summarized in Figure 2. Plug characteristics are controlled by the extent of open-system degassing (equation (2)). Accordingly, increasing magma flow rate decreases plug thickness because increased pressure required to drive higher flow rates delays exsolution of volatiles and shifts open-system degassing to shallower regions of the conduit. Plug density decreases for higher flow rates because open-system degassing occurs over a relatively shorter period during ascent from chamber to surface. For example, for Model B and a bubble connectivity threshold of 60% vesicularity, Q_{vol} = 75 m^3 s^{-1} produces a low-density plug 60 m thick, Q_{vol} = 37.5 m^3 s^{-1} creates a moderate density plug 210 m thick, and Q_{vol} = 7.5 m^3 s^{-1} creates a slightly denser plug 450 m thick. Increasing bubble connectivity threshold decreases plug thickness. For a fixed flow rate (7.5 m^3 s^{-1}), plug thickness varies from 850 m for an assumed bubble connectivity threshold of 45% vesicularity to 50 m for an 80% threshold. Increasing initial total water content or decreasing vertical permeability shifts the entire curve toward lower density. Increasing edifice permeability or increasing the time available for static degassing (Model C) pushes the system toward a dense plug with an abrupt contact between dense rock and underlying vesicular magma. Subsurface overpressure is most sensitive to flow rate, such that increasing flow rate makes conduit overpressure shallower and increases its magnitude and vertical extent (Figure 1c), changes which should increase the magnitude and breadth of surface deformation. This correlation is consistent with observations noted by *Watson et al.* [2000], where during an effusive stage of the SHV eruption, increased gas emissions and deformation magnitude were attributed to increased magma flow rates.

4. Discussion

[18] Model B is most consistent with independent estimates of pre-explosion conduit conditions, however, model simplifications may affect detailed results. For example, we assumed constant k_{cr} with depth due to the paucity of edifice permeability measurements; in reality, permeability likely increases toward the surface, which should lead to a more gradual transition to the dense, degassed magma plug than that exhibited by Model B. In addition, we chose to exclude the effects of bubbles on magma viscosity. Our test runs suggest that general trends and conclusions do not change when bubble-suspension rheology is incorporated. However, detailed results depend strongly on dynamic regime [*Llewellin and Manga*, 2005], which is affected by flow rate, bubble size, and bubble growth style (growth- or nucleation-dominated). We therefore recommend a future numerical study focused exclusively on bubble-suspension rheology, which incorporates detailed analysis of bubbles in natural samples.

[19] Prior to a Vulcanian explosion, overpressure builds beneath a shallow conduit plug. Increasing surface tilt [*Voight et al.*, 1998, 1999] has been cited as evidence for increasing conduit pressure leading to explosions at SHV. *Lensky et al.* [2004] suggest that conduit plugging may allow gas pressure to build as volatiles continue to exsolve from the melt until equilibrium is reached. The magma ascent model used in this study assumes that degassing occurs instantaneously in response to decompression (i.e. equilibrium degassing); however, if there is kinetic delay (i.e. disequilibrium degassing), conduit overpressure could require time to develop. Under disequilibrium degassing conditions, gases will continue to exsolve after magma stagnation and increase conduit pressure via volume increase until an explosion occurs (or the plug is displaced upwards during an effusive phase), possibly explaining the ten-hour repose interval between explosions in 1997 at SHV

and the cyclic nature of Vulcanian explosive behavior in general.

[20] Although our 1D model does not account for horizontal variations, such as shear zones and gas escape pathways parallel to conduit walls, we recognize their potential role in eruptive processes. Once overpressure has developed, two different styles of explosion initiation are envisaged. The first involves shear-induced fragmentation along conduit margins [*Gonnermann and Manga*, 2003; *Tuffen and Dingwell*, 2005] and produces a ring-shaped opening. The central part of the magma plug may remain intact while gas and ash are emitted through the ring-shaped opening, as has been observed at Santiaguito volcano, Guatemala [*Bluth and Rose*, 2004].

[21] The second style initiates by plug fragmentation, as evidenced by ballistics at SHV in 1997 [*Druitt et al.*, 2002]. Plug fragmentation may occur when conduit overpressure exceeds shear resistance along conduit walls and rapidly ejects a portion of the plug from the conduit releasing sufficient confining pressure to cause explosive fragmentation [*Alidibirov and Dingwell*, 1996]. Given that an instantaneous decompression of 5–7 MPa is sufficient to fragment magma with roughly 20% vesicularity or greater [*Spieler et al.*, 2004], explosive eruption may initiate for Model B by a fast ejection of the top ~150 m of the plug, which is underlain by high-pressure magma with >20% porosity. Relatively thin and/or low-density plugs, associated with high magma flow rates, as in Model C, should strongly favor explosion, as only 60 m must be disrupted to expose magma primed for fragmentation. Alternatively, thick, dense plugs associated with low magma flow rates should favor effusion.

5. Conclusions

[22] Three conceptual models for conduit plug formation were tested using one-dimensional numerical models of magma ascent and initial and boundary conditions established for the period of well-documented Vulcanian explosions at the Soufrière Hills volcano in 1997. Model results were compared against geophysical estimates of depth to overpressure and pre-explosion conduit pressure profiles estimated by clast analysis. We conclude that the assumption of steady magma ascent over the course of the repose period, along with vertical and sub-vertical open-system degassing (Model B) reasonably approximates the 1997 explosive period at SHV. According to our model results, a significant increase in system permeability in the upper conduit could explain the formation of a dense conduit plug, a feature typically associated with Vulcanian explosions. In general, plug thickness and density, along with depth and magnitude of overpressure are controlled by magma flow rate, surrounding country rock permeability, and bubble connectivity threshold. Magma flow rate appears to be the most important system parameter, where increasing flow rate increases the magnitude and extent of conduit overpressure, illustrating a relationship between subsurface parameters and overpressure that should prove useful to interpretation of surface deformation data. Increasing magma flow rate also decreases the density and thickness of the confining cap, which may favor explosion over extrusion.

[23] **Acknowledgments.** This research was supported by NSF grant EAR-0310329. We thank two anonymous reviewers for insightful comments.

References

Alidibirov, M., and D. Dingwell (1996), Magma fragmentation by rapid decompression, *Nature*, *380*, 146–148.

Barclay, J., M. R. Carroll, M. J. Rutherford, M. D. Murphy, J. D. Devine, J. Gardner, and R. S. J. Sparks (1998), Experimental phase equilibria constraints on pre-eruptive storage conditions of the Soufrière Hills magma, *Geophys. Res. Lett.*, *25*, 3437–3440.

Belousov, A., B. Voight, M. Belousova, and A. Petukhin (2002), Pyroclastic surges and flows from the 8–10 May 1997 explosive eruption of Bezymianny volcano, Kamchatka, Russia, *Bull. Volcanol.*, *64*, 455–471.

Bluth, G. J. S., and W. I. Rose (2004), Observations of eruptive activity at Santiaguito volcano, Guatemala, *J. Volcanol. Geotherm. Res.*, *136*, 297–302.

Cashman, K. V., and S. M. McConnell (2005), Multiple levels of magma storage during the 1980 summer eruptions of Mount St. Helens, WA, *Bull. Volcanol.*, *68*, 57–75.

D'Oriano, C., E. Poggianti, A. Bertagnini, R. Cioni, P. Landi, M. Polacci, and M. Rosi (2005), Changes in eruptive style during the A.D. 1538 Monte Nuovo eruption (Phlegrean Fields, Italy): The role of syn-eruptive crystallization, *Bull. Volcanol.*, *67*, 601–621.

Druitt, T. H., et al. (2002), Episodes of cyclic vulcanian explosive activity with fountain collapse at Soufrière Hills volcano, Montserrat, *Geol. Soc. London Mem.*, *21*, 281–306.

Eichelberger, J. C., C. R. Carrigan, H. R. Westrich, and R. H. Price (1986), Non-explosive silicic volcanism, *Nature*, *323*, 598–602.

Gonnermann, H. M., and M. Manga (2003), Explosive volcanism may not be an inevitable consequence of magma fragmentation, *Nature*, *426*, 432–435.

Hammer, J. E., K. V. Cashman, R. P. Hoblitt, and S. Newman (1999), Degassing and microlite crystallization during pre-climactic events of the 1991 eruption of Mt. Pinatubo, Philippines, *Bull. Volcanol.*, *60*, 355–380.

Heiken, G., K. Wohletz, and J. Eichelberger (1988), Fracture fillings and intrusive pyroclasts, Inyo Domes, California, *J. Geophys. Res.*, *93*, 4335–4350.

Hess, K. U., and D. B. Dingwell (1996), Viscosities of hydrous leucogranitic melts: A non-Arrhenian model, *Am. Mineral.*, *81*, 1297–1300.

Jaupart, C., and C. J. Allègre (1991), Gas content, eruption rate and instabilities of eruption regime in silicic volcanoes, *Earth Planet. Sci. Lett.*, *102*, 413–429.

Klug, C., and K. V. Cashman (1996), Permeability development in vesiculating magmas: Implication for fragmentation, *Bull. Volcanol.*, *58*, 87–100.

Lejeune, A. M., Y. Bottinga, T. W. Trull, and P. Richet (1999), Rheology of bubble-bearing magmas, *Earth Planet. Sci. Lett.*, *166*, 71–84.

Lensky, N. G., O. Navon, and V. Lyakhovsky (2004), Bubble growth during decompression of magma: Experimentally and theoretical investigation, *J. Volcanol. Geotherm. Res.*, *129*, 7–22.

Llewellin, E. W., and M. Manga (2005), Bubble suspension rheology and implications for conduit flow, *J. Volcanol. Geotherm. Res.*, *143*, 205–217.

Melnik, O., and R. S. J. Sparks (1999), Nonlinear dynamics of lava dome extrusion, *Nature*, *402*, 37–41.

Melnik, O., and R. S. J. Sparks (2002a), Dynamics of magma ascent and lava extrusion at Soufrière Hills Volcano, Montserrat, *Geol. Soc. London Mem.*, *21*, 153–171.

Melnik, O., and R. S. J. Sparks (2002b), Modelling of conduit flow dynamics during explosive activity at Soufrière Hills Volcano, Montserrat, *Geol. Soc. London Mem.*, *21*, 307–317.

Melnik, O., A. A. Barmin, and R. S. J. Sparks (2005), Dynamics of magma flow inside volcanic conduits with bubble overpressure buildup and gas loss through permeable magma, *J. Volcanol. Geotherm. Res.*, *143*, 53–68.

Morrissey, M. M., and L. G. Mastin (2000), Vulcanian eruptions, in *Encyclopedia of Volcanoes*, edited by H. Sigurdson et al., pp. 463–476, Elsevier, New York.

Murphy, M. D., R. S. J. Sparks, J. Barclay, M. R. Carroll, A. M. Lejeune, T. S. Brewer, R. Macdonald, S. Black, and S. Young (1998), The role of magma mixing in triggering the current eruption at the Soufrière Hills volcano, Montserrat, West Indies, *Geophys. Res. Lett.*, *25*, 3433–3436.

Saar, M. O., and M. Manga (1999), Permeability-porosity relationship in vesicular basalts, *Geophys. Res. Lett.*, *26*, 111–114.

Sparks, R. S. J. (1997), Causes and consequences of pressurisation in lava dome eruptions, *Earth Planet. Sci. Lett.*, *150*, 177–189.

Spieler, O., B. Kennedy, U. Kueppers, D. B. Dingwell, B. Scheu, and J. Taddeucci (2004), The fragmentation threshold of pyroclastic rocks, *Earth Planet. Sci. Lett.*, *226*, 139–148.

Stix, J., C. R. Torres, M. L. Narváez, J. G. P. Cortés, A. J. Raigosa, M. D. Gómez, and R. Castonguay (1997), A model of Vulcanian eruptions at Galeras volcano, Colombia, *J. Volcanol. Geotherm. Res.*, *77*, 285–303.

Taddeucci, J., M. Pompilio, and P. Scarlato (2004), Conduit processes during the July–August 2001 explosive activity of Mt. Etna (Italy): Inferences from glass chemistry crystal size distribution of ash particles, *J. Volcanol. Geotherm. Res.*, *137*, 33–54.

Takeuchi, S., S. Nakashima, A. Tomiya, and H. Shinohara (2005), Experimental constraints on the low gas permeability of vesicular magma during decompression, *Geophys. Res. Lett.*, *32*, L10312, doi:10.1029/2005GL022491.

Tuffen, H., and D. Dingwell (2005), Fault textures in volcanic conduits: Evidence for seismic trigger mechanisms during silicic eruptions, *Bull. Volcanol.*, *67*, 370–387.

Voight, B., R. P. Hoblitt, A. B. Clarke, A. B. Lockhart, A. D. Miller, L. Lynch, and J. MacMahon (1998), Remarkable cyclic ground deformation monitored in real time on Montserrat and its use in eruption forecasting, *Geophys. Res. Lett.*, *25*, 3405–3408.

Voight, B., et al. (1999), Magma flow instability and cyclic activity at Soufrière Hills Volcano, Montserrat, *Science*, *283*, 1138–1142.

Watson, I. M., et al. (2000), The relationship between degassing and ground deformation at Soufrière Hills Volcano, Montserrat, *J. Volcanol. Geotherm. Res.*, *98*, 117–126.

Widiwijayanti, C., A. B. Clarke, D. Elsworth, and B. Voight (2005), Geodetic Constraints on the Shallow Magma System at Soufrière Hills Volcano, Montserrat, *Geophys. Res. Lett.*, *32*, L11309, doi:10.1029/2005GL022846.

Wilson, L., R. S. J. Sparks, and G. P. L. Walker (1980), Explosive volcanic eruptions: IV. The control of magma properties and conduit geometry on eruption column behavior, *Geophys. J. R. Astron. Soc.*, *63*, 117–148.

A. B. Clarke and K. Diller, School of Earth and Space Exploration, Arizona State University, Tempe, AZ 85287-1404, USA. (amanda.clarke@asu.edu; kristi.diller@asu.edu)

A. Neri, Sezione di Pisa, Istituto Nazionale di Geofisica e Vulcanologia, Pisa I-56126, Italy. (neri@pi.ingv.it)

B. Voight, College of Earth and Mineral Sciences, Pennsylvania State University, University Park, PA 16802, USA. (voight@ems.psu.edu)